10

Integrated precision measurement of optical characteristics of serial indium phosphide wafers

© L.A. Fedyukhin[1], E.A. Kolosovsky[1], A.V. Gorchakov[2]

[1] Rzhanov Institute of Semiconductor Physics, Siberian Branch, Russian Academy of Sciences, Novosibirsk, Russia
[2] Novosibirsk State University, Novosibirsk, Russia

E-mail: leogal2007@mail.ru

Received June 06, 2024
Revised October 27, 2024
Accepted November 18, 2024

Precision measurement of optical characteristics of serially produced indium phosphide wafers, including thickness, refractive indices of the substrate and transition layers, absorption of the transition layer, was performed. The measurements were carried out using the method of invariants at a light wavelength of 1549.14 nm. A detailed analysis of the target function revealed the presence of regular regions of localization of the target function values — pockets. The width of the pockets, the period, the relationship with the parameters determining the number of minima of the angular distributions of the transmission coefficients were determined. Confidence intervals of the measured values of the optical parameters were calculated using indium phosphide as an example.

Keywords: classical optics, interferometry, refractive index, Fabry-Perot interferometer, method of invariants.

DOI: 10.61011/EOS.2024.12.60452.6765-24

Introduction

Getting the accurate values of the refractive index for transparent materials is critical for design and manufacturing of many optic devices, which includes design of high-resolution optic devices, large numerical aperture, with minimum spherical and chromatic aberrations [1], lasers with the vertical radiation on the surface of the resonant cavity [2], light-emitting and superluminescent diodes [3], photodetectors [4], photovoltaic devices [5], thin-film multi-layer structures, such as antiglare coatings with high reflectivity and other spectral interference filters [6]. The value of the refractive index dispersion (Sellmeier equation) of non-linear crystals is important for design of frequency conversion devices. For these applications the crystal refractive index must be known with the accuracy of 0.0001 [7]. High demand for the accuracy of the substrate refractive index is important for calculation of the integral optics elements [8–11].

The first data on the indium phosphide refractive index are from 1965 [12]. The values are given for the wavelength range from 1200 nm to 1600 nm. [13] reports the value of the refractive index for an InP film grown on a n-doped substrate with carrier concentration to level $2 \cdot 10^{18}\,\mathrm{cm}^{-3}$, and its interconnection with the density of the charge carrier in the substrate conduction band. [14,15] using the method of multi-angle ellipsometry in the area of the Brewster angle measured the refractive indices of the substrate of indium phosphide and its oxide. The presence of the natural indium phosphide oxide on the surface is discussed in [16]. We find publication [17] important, which gives the results of the temperature dependences of Si, GaAs and InP wafer refractive indices relative to their values at room temperature.

Interference methods for measurement of the refractive indices of the optical materials are found to be most accurate [18,19]. Multiple rereflections in the interferometer cause unlimited increase in the length of light interaction with the material, which provides for high accuracy in determination of material parameters by interference methods. This is the method used to measure the refractive indices of standards [20]. There are two types of interference methods — absolute and relative. The absolute method is in fact the method to measure light velocity in the specimen material. The relative interference method is based on comparison of the interferograms of the standard, with its refractive index measured by the absolute interference method, and of the specimen. Both methods require high precision knowledge of both the length of light interaction with the material and the value of the probing radiation wavelength. It is critical to account for the transition layers between the contacting media [21,22]. An error, depending on the selected method, may reach 10%, which is not acceptable for design of integral-optical circuit chips. It is also necessary to keep in mind the potential dependence of the measured parameters on the substrate thickness, since the phase length (the number of wavelengths fitting on the thickness of the sample D with the refractive index n) for the wafers used to develop integral-optical elements $Dn/\lambda < 10^3$.

The minimization approved by all parameters (calculation of the structure parameters using experimental data) is a rather complicated task, and for its solution it is necessary to develop a specialized algorithm. The role of numerical experiments that explain the transformation of

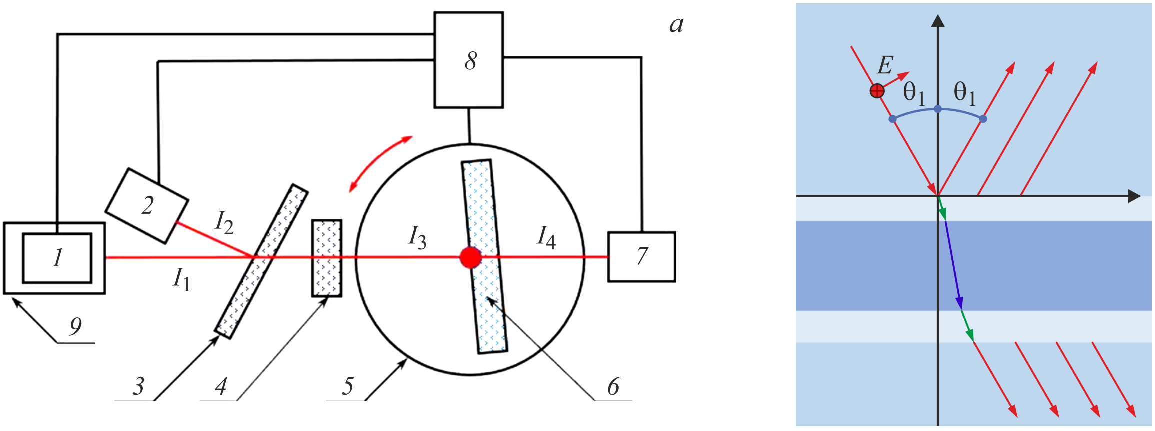

Figure 1. (*a*) Measurement bench diagram. *1* — solid-state single-frequency laser BLD-1550-BF-20, *2, 7* — IC photodetectors PM-100, *3* — wedge-shaped beam splitter, *4* — Glan prism, *5* — alignment unit based on software controllable turn table Thorlabs HDR50, *6* — specimen, *8* — automated unit to control the alignment unit and to record the measured parameters, *9* — unit of temperature stabilization of the laser diode; (*b*) scheme that explains the location of the layers in a model of a five-layer symmetrical structure. The transmission of the beams is shown with the arrows. Designation of layers from the top to the bottom: refractive indices $\{n_1 = 1, \tilde{n}_2, n_3, \tilde{n}_2, n_1 = 1\}$; thicknesses $\{d_1 = \infty, d_2, d_3, d_2, d_1 = \infty\}$.

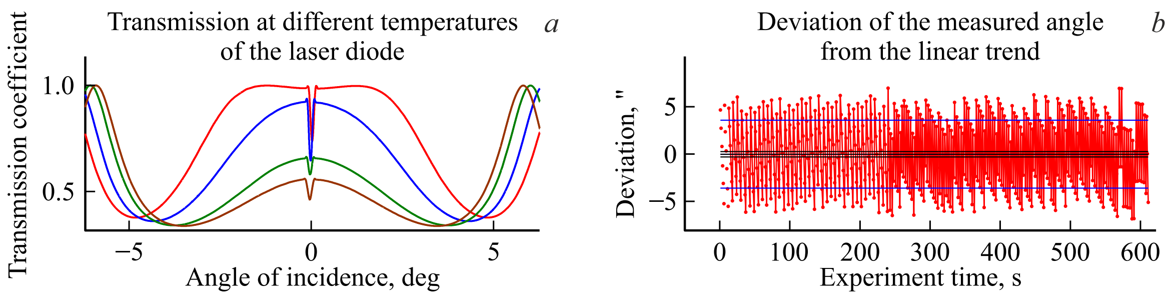

Figure 2. (*a*) Angular dependence of the transmission ratio near the normal line at the temperature of laser diode +19°C (red line), +23°C (blue), +25°C (green), +27°C (brown); (*b*) deviation of the sample rotation angle from the linear trend in angular seconds.

the target function in process of minimization increases. A question arises in the selection of parameters that most clearly represent this transformation. The objective of this paper is exactly this complex approach to measurements and calculation of the main optical characteristics of materials implemented experimentally on the indium phosphide wafers. The measurements were made at the light wavelength $\lambda = 1549.14$ nm at temperature 23°C on InP wafers of serial production using the absolute interference method — method of invariants [21]. The experimental results were processed on the basis of a mathematical model of symmetrical five-layer structure.

Interference refractometer of absolute type

Measurements of the interference pattern with light transmission through the sample were made on the bench, the principal diagram of which is shown in fig. 1, *a*. The main element of the optical part in the diagram is the alignment unit *5* with a measured object *6* fixed on its platform. The alignment unit design provides for the following:

• ability to match the working surface of the structure with the platform rotation axis (designated with a red point in fig. 1, *a*);

• location of the optical axis in the plane perpendicular to the working surface of the structure;

• match of the optical axis from the source of probing radiation *1* with the platform rotation axis;

• variation of the angles of probing radiation incidence on the specimen in the range $\sim 180°$.

A beam of light linearly polarized in the incidence plane (*p*-wave), from a single-frequency source of radiation, directed along the optical axis, passes through the wedge-shaped beam splitter *2*, Glan prism *4*, specimen *6*. Its intensity is measured with photodetectors *2* and *7*. The program unit *8* controls the rotation of the alignment unit platform *5*, records the measured values, calculates the optical parameters of the structure.

The source of light used was a solid-state single-frequency laser BLD-1550-BF-20, with external programmable unit of temperature stabilization Thorlabs TTC001, which provides for the maintenance of the laser working zone temperature at the level of $(18.0 \pm 0.1)^\circ$C. Such stabilization is important, since the preliminary experiments recorded a substantial impact of the laser diode temperature and the resulting change of the emitter wavelength at the angular distributions of the transmission coefficients (fig. 2, *a*).

Direct measurement of the light wavelength using high-precision meter *Ångstrom Laser Spectrum Analyzer (LSA), Hifinesse Japan K.K.*, Japan, confirmed the data sheet values of the laser diode: $\lambda = 1549.14$ nm, $\Delta f = 200$ kHz, however, could not provide the confirmed value of the wavelength for temperature variation. Results shown in fig. 2, *a* demonstrate high sensitivity of the transmission coefficient to the laser radiation wavelength, substantially exceeding the resolution of the high-precision meter *Ångstrom LSA*.

The advantage of the proposed optical scheme is the use of geometry for transmission. In this case the light spot of the beam that passed through the specimen is practically stationary and does not go beyond the photodetector aperture when the specimen rotates. Besides, the plane-parallel wafer of the sample in this scheme is itself a Fabry-Perot resonant cavity. This substantially reduces the level of noise signals caused by tiniest specimen vibrations. Intensities of incident light and light transmitted through the sample were measured simultaneously by two IR photodetectors PM-100. In the beginning of every experiment the calibration coefficient of the optical scheme K was measured, which is equal to the ratio of intensities I_3/I_{2off}, recorded by photodetectors *2* and *7* (fig. 1, *a*), in the absence of the sample. This made it possible to substantially reduce the effect of the emitter intensity drift and to record the actual specimen transmission coefficient at the output: $T = (I_4/I_{2on})/K$.

The bench testing showed the following: aperture of the probing radiation on the working surface of the specimen by level $1/e$ is ~ 2 mm; divergence of the beam $\sim 2 \cdot 10^{-3}$ rad; the ellipticity of radiation after transmission through the Glan prism was $\sim 2 \cdot 10^{-4}$, the standard deviation of the calibration coefficient of the optical scheme K from the time-average one did not exceed 10^{-4}. The dynamic range of transmission coefficient measurement ~ 80 dB. The temperature of the room with the measurement bench was measured with a sensor located near the sample. During the experiment (~ 600 s) the temperature variation did not exceed 0.2°C at average temperature of 23.0°C.

Fig. 2, *b* shows the deviation of the sample rotation angle measured in the experiment from the linear trend. The measurements were made at equal time intervals (reference points in 1 s). The angles between the reference points were calculated under the assumption of a constant angular velocity of the platform. The transmission ratio was also measured at equal intervals of time. The used scheme practically excluded the effect of the platform rotation irregularity *5* (fig. 1, *a*). The black lines in fig. 2, *b* indicate a confidence interval in the measurement of angles amounting to less than 0.3 angular seconds. The blue lines indicate a standard deviation.

Mathematical model

The theoretical basis for the operation of the interference refractometer of absolute type is a well developed section of the optics of light interaction with multilayer plane-parallel structures [23,24], being at the same time the Fabry-Perot interferometers [25]. It is known [26] that for the wafers with the ideal interfaces, when the thickness of transition layers is zero, there is an invariant connection between angles $\theta = [\theta_1, \ldots \theta_q]$, defining the position of the minima of reflection coefficients/maxima of the transmission coefficient in the interferogram:

$$\begin{cases} Inv_\varepsilon = \sin^2\theta_q - \frac{(4\sin^2\theta_{q+1} - 3\sin^2 q - \sin^2\theta_{q+2})^2}{8(\sin^2\theta_{q+2} - 2\sin^2\theta_{q+1} + \sin^2\theta_q)}, \\ Inv_d = 2\sin^2\theta_{q+1} - \sin^2\theta_q - \sin^2\theta_{q+2}. \end{cases}$$

Values Inv_ε and Inv_d are permanent for this material, do not depend on number q of the interference minimum and may be calculated by the measurement of the angular position in three nearest interference minima θ_q. This makes it possible to directly and independently calculate both the refractive index and the wafer thickness:

$$n_3 = n_1\sqrt{Inv_\varepsilon}, \quad d_3 = \frac{\lambda}{\sqrt{2Inv_d}}.$$

However, the multiple attempts of the authors to use this property of the plane-parallel wafers failed. The results of calculation based on the experimental data were substantially different from the expected values both for the refractive index and for the wafer thickness. A similar situation occurs when trying to measure the refractive index by the reflection coefficient near the normal, as well as near the Brewster angle [22]. The conclusion is unambiguous — the model of ideal interfaces must be supplemented with transition layers taking into account the features of the real structure interfaces. For plane-parallel wafers this leads to a five-layer structure model. In the case when both surfaces are treated using the same technology — to a symmetrical five-layer structure (fig. 1, *b*). The middle layer models the material, for which it is necessary to obtain the value of the refractive index. The transition layers *2* and *4* take into account the features of the real structure interfaces with the environment (layers *1* and *5*). The angular distributions of the reflection coefficients provide the recurrent formulas for m-layer structures [23,24]

$$R_m = |r_m|^2 = \left| \frac{g_{m,m-1} + r_{m-1}\exp(-i\beta_m d_m)}{1 + g_{m,m-1} r_{m-1}\exp(-i\beta_m d_m)} \right|^2.$$

Here r_m — generalized Fresnel coefficients,

$g_{m,m-1} = \frac{n_m\cos\theta_{m-1} - n_{m-1}\cos\theta_m}{n_m\cos\theta_{m-1} + n_{m-1}\cos\theta_m}$ — classic Fresnel coefficients for a p-wave,

$\beta_m = \frac{4\pi}{\lambda} n_m \cos\varphi_m$ — phase length of m-th layer.

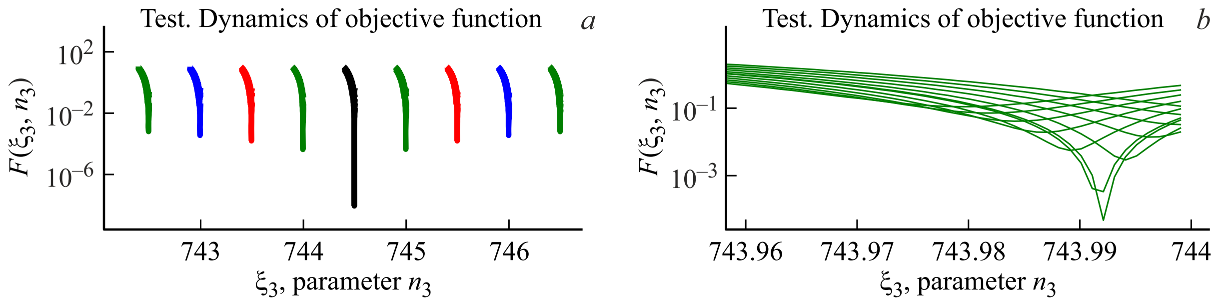

Figure 3. (*a*) Target function dynamics. Curve family parameter — n_2 (black indicates the zero pocket); (*b*) target function dynamics in the minus one pocket.

It would be reasonable to assume that thin transition layers hardly affect the invariant ratios and extrema of the angular distributions of reflection/transmission coefficients will make it possible to unambiguously recover the structure parameters.

Target function. Pockets

To test the suggested assumption, a numerical experiment was done, where the observed parameters were a vector line of extrema of the transmission coefficient for a light wave polarized in the incidence plane — $\theta^t = (\theta_1^t, \theta_2^t \ldots \theta_m^t)$, for a test symmetrical five layer structure with the parameters: refractive indices of layers — $\{n_1^t, n_2^t, n_3^t, n_4^t, n_5^t\} = \{1.0, 2.8, 3.16, 2.8, 1.0\}$; thicknesses — $\{d_2^t, d_3^t, d_4^t\} = \{100, 365000, 100\}$ nm. The probing radiation wavelength is $\lambda = 1549.244$ nm.

To solve the task at hand, it is necessary to minimize the target function

$$F(d_i, n_i) = |\theta^t - \theta(d_i, n_i)|^2, \tag{1}$$

representing a sum of squared deviations from the position of the extrema of the test — θ^t and sample — θ structures. Summation in (1) occurs exclusively by the angular position of the extrema. The amplitudes of the transmission coefficient being a substantial source of errors do not participate in the calculation. Moreover, the numerical calculations show that the position of the extrema hardly depends on such parameters of diffraction divergence of the light beam and presence of absorption in the transition layers. The expected values of the confidence intervals for all the parameters of the structure determined by the interference methods are $\sim 10^{-7}$. It is clear that it is complicated to determine the minimum of the target function of the four variables by simple searching — the phase space volume is rather large. Number of points to be processed exceed 10^{20}. Let us analyze the dynamics of target function minimization for the simplest case, when the test structure consists of three layers ($d_2^t = d_4^t = 0$). Minimization is carried out according to two parameters of the trial structure — refractive index n_3 and dimensionless parameter $\xi_3 = \frac{d_3 n_3}{\lambda}$ — number of wavelengths at normal transmission through a layer with thickness of d_3 and refractive index n_3. It is important to note that parameter ξ_3 is unambiguously related to the absolute number of the first interference minimum from the normal line for the angular distribution of the transmission coefficient [25]:

$$m_{\max} = \left\lfloor 2\frac{d_3}{\lambda} n_3 \right\rfloor = \lfloor 2\xi_3 \rfloor, \tag{2}$$

and also defines the number of interference minima of the angular distribution:

$$N = m_{\max} - m_{\min} = \lfloor 2\xi_3 \rfloor - \left\lceil 2\xi_3 \sqrt{1 - \frac{n_1^2}{n_3^2}} \right\rceil. \tag{3}$$

Here $m_{\min} = \left\lceil 2\frac{d_3}{\lambda} n_3 \right\rceil = \lfloor 2\xi_3 \rfloor$ — the absolute number of the last interference minimum of the angular distribution of the reflection coefficient.

The results of numerical calculations are shown in fig. 3.

We can see that values $F(\xi_3, n_3)$, as function of xi_3 (fig. 3, *a*), are localized in rather narrow periodically located pockets. The minima of each pocket are implemented at various values of parameter n_3 (fig. 3, *b*).

With a change in ξ_3 the value $m_{\max}$ remains constant in a certain range or „pocket“, until the integer portion of $2\xi_3$ changes by one. Therefore, the pocket width by ξ_3 is 0.5. The total number of the interferogram minima in the pocket remains constant, too — N. Moreover, integer solutions to equation (3) when going to the adjacent pockets contain a significant part of values N, equal to its value in the zero pocket, the borders of which are indicated with black vertical lines in fig. 4, *a*.

The numerical calculation shows that the minima of pockets are located strictly periodically, with a period equal to the double width of the pocket — one. The global minima of the target function are formed with the equality of the absolute numbers $m_{\max}$ and $m_{\min}$ of the test and sample structures. To form a local minimum in the pockets it is sufficient that the total quantity of interferogram minima coincide — N. The parameters of the structure determined by each pocket ($d_3^{\min}, n_3^{\min}$) differ significantly from each

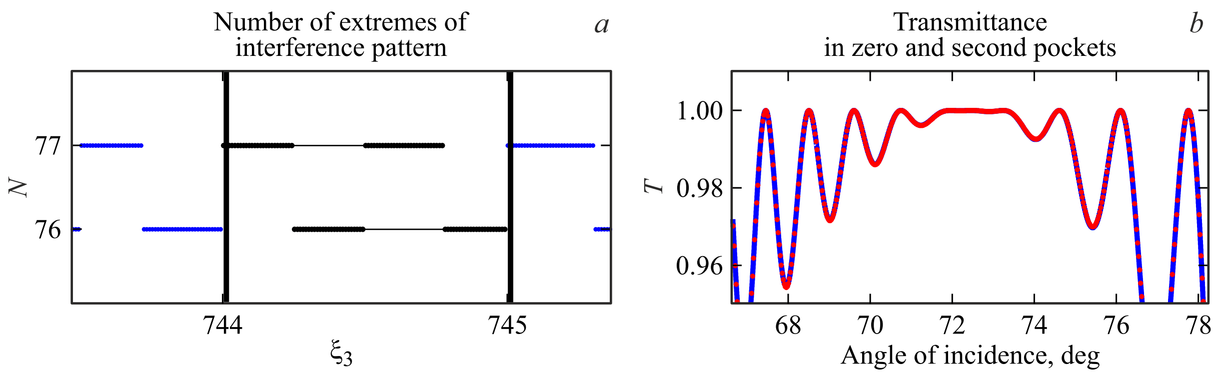

Figure 4. (a) Number of interferogram extrema; (b) transmission coefficient at parameters defined by zero (blue line) and second (red dotted line) pockets (table. 1).

Table 1. Values of parameters produced by algorithm of minimization in various pockets

Pocket	$m_{\max}$	d_3, nm	n_3
−2	149	364 748	3.15
−1	148	364 874	3.15
0	148	365 000	3.16
1	148	365 126	3.16
2	148	365 251	3.16

other (table 1). At the same time the angular distributions of the transmission coefficient and the position of the extrema are hardly distinguishable (fig. 4, b).

Such „similar" structures were reported previously [27]. Their presence prevents the experimenter from obtaining an unambiguous result of minimization. Only in the case when the value of the target function in the minimum is substantially lower than its value in several adjacent pockets, the experimenter may believe in good faith that the values obtained by minimization are valid. Otherwise it is necessary to involve the additional data, in particular, the results of the direct measurement of structure thickness with the necessary confidence interval determined between the minima in the adjacent pockets. Minimization by parameter ξ_3 has the practical value too, since it does not require the knowledge of the probing radiation wavelength. However, one should remember that the parameter defined in this manner is fair in the narrow range of light wavelengths, when you can neglect the dispersion of the refractive index. Note an important detail. The transmission interferogram may have an „extra minimum", compliant with the full polarization angle. In virtue of this circumstance some minima near the expected Brewster angle should be excluded from the minimization process.

Presence of thin transition layers $d_2^t, d_4^t \neq 0$ essentially changes nothing in the behavior of the target function (fig. 3). The difference is the presence of additional local minima in each of the pockets at multiple values of parameter $\xi_2 = \frac{d_2}{\lambda} n_2$ (fig. 5). The frequency of minima in them is not strict. In the area of one pocket (either of four) the target function is monotonically concave (fig. 5, b), which substantially facilitates searching for the minimum.

The dependences shown in fig. 5 convince that the logic confidently determines the only minimum in the estimated range of parameters. In the vicinity of the minimum the value of the target function reduces monotonically as the sample parameters of the structure approach the test values (fig. 5, b). The dynamics of the target function with the presence of the normally distributed noise additive (fig. 5, c) indicates algorithm's resistance to measurement errors. The conducted numerical experiment confirms the above hypothesis that the vector-string of the angular position of the transmission coefficient θ^t extrema contains sufficient information to recover the optical parameters of the structure.

As a rule, the measurement of the angular position of the interference minima contains the systematic error related to the definition of the angle compliant with the normal incidence of the radiation on the sample. This systematic error may be minimized by adding a small correction ϕ_N to the normal line angle in the list of the varied parameters. The remaining tapering of the measured structure is also a source of a systematic error. To minimize it, the sample position must be selected so that the axis (rib) of the wedge is parallel to the incidence plane. The transition layers may be the area of the radiation absorption. This dictates the need to include an imaginary additive into the model to the refractive index of the transition layer: $\tilde{n}_2 = n_2 + ik_2$. Therefore, the logic of minimization in the model of a symmetrical five layer structure includes minimization of the target function by six parameters $\{n_2, d_2, n_3, d_3, k_2, \phi_N\}$.

Experiment

Measurement object — indium phosphide wafer of serial production, which is a quarter of the disc with thickness of

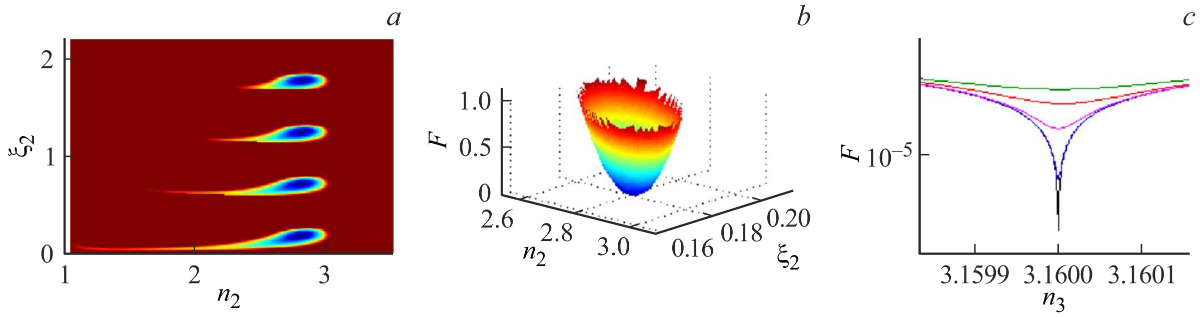

Figure 5. (*a*) Color chart of target function in coordinates ξ_2, n_2; (*b*) target function in the pocket minimum area, (*c*) target function dynamics with presence of noise additives with amplitude $\delta = 0$ (black line), $1''$ (blue line), $10''$ (purple line), $30''$ (red line), $60''$ (green line).

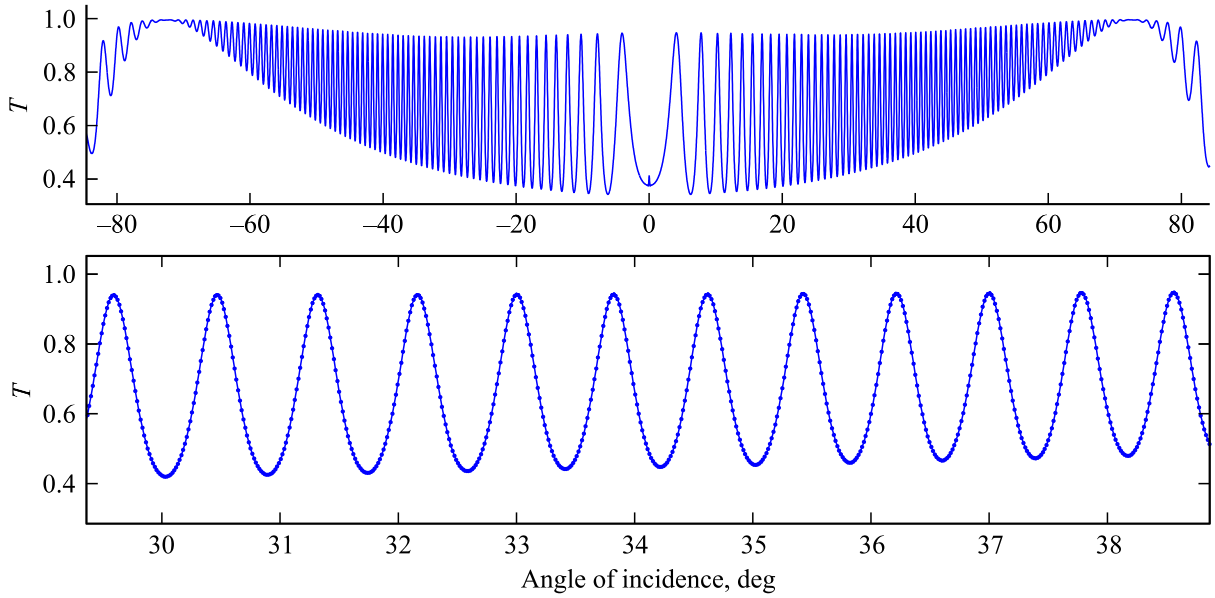

Figure 6. Experiment. Angular distribution of the transmission coefficient obtained by measurement in the interference refractometer of absolute type.

360 μm, diameter of 50 mm. These are exactly the wafers used to produce integral-optical devices. Fig. 6 shows the angular distribution of the transmission coefficient obtained by measurement according to the scheme for the above interference refractometer of absolute type.

The distribution contains more than 12 thousand points of the transmission coefficient values that are equidistant by incident angle, indicating 306 extrema. Their angular position corresponding to the right branch of the interferogram, is shown in fig. 7, *a*. The extrema with numbers from 1 to 137 and from 144 to 151 were accepted for processing. The extrema in the Brewster angle area (numbers from 138 to 143) were excluded for the reason of potential presence of the „extra minimum", corresponding to the expected Brewster angle of the substrate. The results shown in fig. 6 indicate that the actions aimed at increasing the sharpness of the interferogram yielded a positive result.

Minimization (search for parameters in the model of the symmetrical five-layer structure that corresponds best to the experiment) was carried out using the scheme of the above numerical experiment. Fig. 8, *a* shows the curve of the target function $F(\xi_2)$ at various values of the parameter n_2. Each of five pockets determines the set of five parameters meeting the minimum value of the target function in the pocket (table 2). The global minimum (pocket 2) determines the structure parameters. Note that the parameters of the transition layer thicknesses determined by the interference method are much lower than the light wavelength. This is caused by properties of the Fabry-Perot interferometer, where the length of light interaction with the material (optical length) increases many times at the expense of multiple rereflections.

Target function dynamics near the second pocket is shown in fig. 8, *b* as function ξ_2 at various values of parameters ξ_3, n_2, n_3. As you can see, the change of

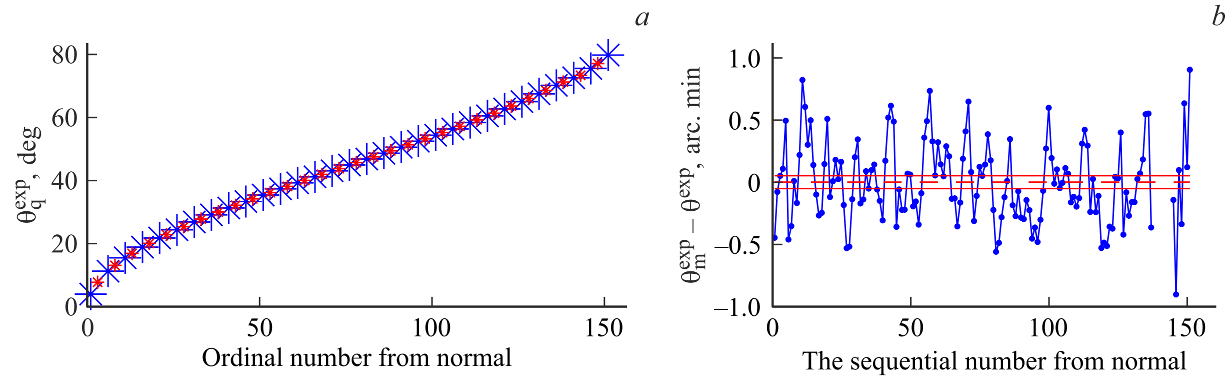

Figure 7. (a) Extrema of the right branch of transmission coefficient are marked with blue. Extrema obtained by minimization are marked with red; (b) deviation in the angular position of the extrema recorded experimentally from their estimated values.

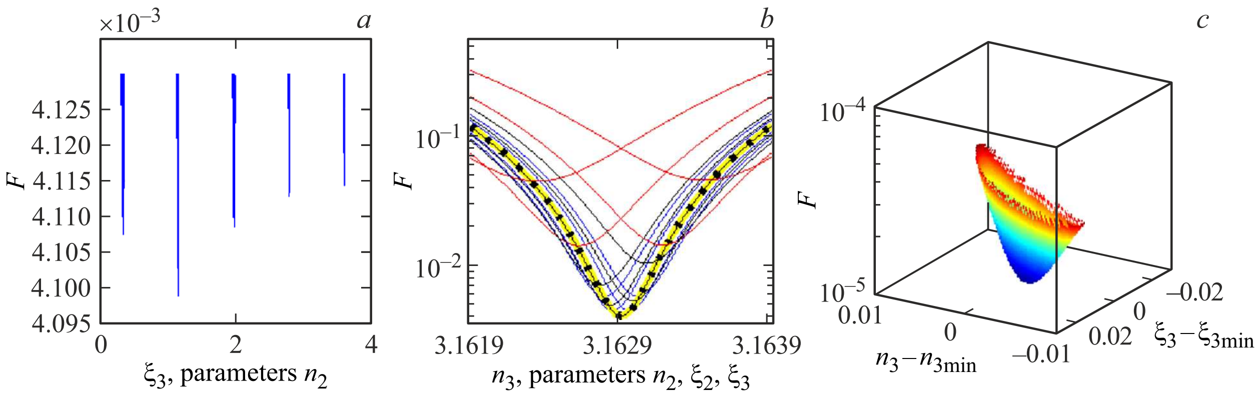

Figure 8. (a) Target function in coordinates $F(\xi_2)$, parameter n_2; (b) target function dynamics in the second pocket minimum. Family of n_2 parameter curves is shown with red color, for parameter n_3 — with blue, parameter ξ_3 — with black. The yellow dotted line highlights the common curve for all families; (c) target function in the pocket minimum area.

Table 2. Values of parameters in the model of the symmetrical five-layer structure obtained by minimization logic in various pockets

№	1st pocket	2nd pocket	3rd pocket	4th pocket	5th pocket
d_2, nm	108.4	371.9	633.6	894.3	1154.6
d_3, nm	366740.0	366208.9	365681.7	365157.1	364633.8
n_2	3.122448	3.122819	3.123000	3.123086	3.123333
n_3	3.162794	3.162884	3.162971	3.163053	3.163129
k_2	0.0025	0.001	0.0004	0.00028	0.00024
NevD, nm	22.7	18.6	14.7	11.4	8.8

any parameter ξ_2, ξ_3, n_2, n_3 causes monotonic growth of the target function, which indicates the absolute nature of the minimum in the pocket. Angular positions of extrema calculated by parameters of minimization in each pocket practically coincide to each other and to the experimental values (fig. 7, a), which indicates similarity of the structures defined by these pockets. It should be noted that within the method the parameters of the structure in table 2 in the pockets differ quite significantly. There can be no other values that are intermediate between the specified ones. The method determines the discrete set of parameters.

Norte that the model used in the calculations has a stepped profile of the refractive index with clear borders (fig. 1, b). Parameters of the transition layer determined on the basis of the experimental data are of course „effective“. In reality the parameters are blurred. Their position may only be indicated conditionally — with effective values. The thickness of the transition layer becomes conditional

Table 3. Optical characteristics of a series InP wafer

Parameter	Value
Light wavelength, nm	1549.14 ± 0.01
Transition layer thickness, nm	371.9 ± 0.2
Substrate thickness, nm	366208.9 ± 0.3
Refractive index of transition layer	3.123 ± 0.003
Refractive index of substrate	3.162884 ± 0.000002
Absorption in transition layer	0.0010 ± 0.0001
Target function minimum	0.0040987

too. This is the conditional value of the transition layer thickness that complies with the one measured by the absolute interference method in the experiment in the model of the symmetrical five-layer structure.

The last row of table 2 provides the value of the structure thickness discrepancy relative to the value measured experimentally by the method of invariants: $\mathrm{NevD} = \mathrm{D_{exp}} - (d_3 + 2d_2)$. For determination of $\mathrm{D_{exp}}$ the authors used a micrometer. The sample was pressed between the micrometer head and the hemisphere aligned to it with diameter of 5 mm. The measurement was done with the method of multiple measurement of thickness in various points of the structure in the light beam incidence area. This made it possible to determine the average value, the standard deviation and the confidence interval of the structure thickness values: $\mathrm{D_{exp}} = 366.93 \pm 0.02\,\mu$m. The same value obtained by the method of invariants is $\mathrm{D} = d_3 + 2d_2 = 366952.7 \pm 0.3$ nm $= 366952.7 \pm 0.0003\,\mu$m (table 3). We can see that the confidence interval when thickness is measured by a micrometer is nearly an order higher than the confidence interval when measured by the method of invariants. Therefore, the absolute interference method of invariants is a rather precise contactless method for measurement of the thickness of plane-parallel wafers in the practically important range from the units of microns to several millimeters, when the high quality interferogram is observed.

Confidence intervals of measured parameters

The important aspect of the method claiming to measure the material parameters is calculation of the confidence intervals. In our case the issue is complicated by the fact that the measured parameter is only the incident angle, and the confidence interval must be calculated for each of the parameters — $\{n_2, d_2, n_3, d_3\} \equiv \{h_i\}$. Angular position of the extremum is the function of its number and parameters of the structure: $\theta_q = F(h_i)$. Change of any parameter h_i causes extremum shift. Shift differential:

$$\Delta\theta_m = \Delta F(h_i) = \Sigma_i \frac{\partial F}{\partial h_i} \Delta h_i = \Sigma_i b_i \Delta h_i.$$

Local derivatives determine the coefficients of linear regression b_i. They show the speed and sign of extremum shift by one variable with the fixed values of the others. Calculation based on the model of the five-layer symmetrical structure with parameters obtained by minimization (table 3, pocket 2) indicates that all regression coefficients are $b_i > 0$. In this case let us assume $\Delta h_i = \Delta\theta_q(h_i)/b_i$ as the top estimate of the differentials $\{\Delta h_i\}$. The confidence interval by level 0.95 for parameters h_i is obtained by the numerical calculation of the differential for 91th extremum, at which the changes are maximal $\theta_{91} = 50.57°$. The experimental value of the confidence interval (in the angular minutes) is calculated by the deviation of the experimental position of the extrema from the values obtained by minimization. It is noted with red solid lines in fig. 7, *b*. The values of the structure parameters determined by the second pocket are given in table 3.

Conclusion

The complex precision measurement of optic characteristics of the serial indium phosphide wafer was peformed. The detailed analysis of the target function dynamics was completed, which made it possible to introduce a concept of pockets — areas of localization of the target function values. A width of pockets is found, as well as the period of localization, connection to the parameters defining the quantity of the minima of the angular distributions of the transmission coefficients. The possibility of recovering the optic parameters of the materials is proven exclusively by measurement of the transmission coefficient extrema without involvement of data on the structure thickness. The conducted analysis made it possible to build the effective logic for target function minimization, which unambiguously recovers five parameters of the material with high precision — absolute refractive index of the substrate, absolute refractive index of the transition layer, substrate thickness, transition layer thickness, transition layer absorption coefficient. The paper estimated the confidence intervals of indium phosphide optical parameters.

The interference scheme with the external resonator requires extreme caution in operation [25]. The proposed and successfully tested scheme of the absolute interference refractometer is less sensitive to the finest vibrations of the optical scheme elements, since the Fabry-Perot resonant cavity is the sample itself. The produced interferogram is notable for its high contrast. The optical scheme of the interference refractometer of absolute type (fig. 1, *a*) may be implemented also as an individual optical instrument.

The conducted measurements confirm the promising outlook of the method of invariants for the efficient measurement of material refractive indices, including for the materials with high values of the refractive indices. The availability of the transition layer with „effective" thickness value 371.9 ± 0.2 nm is found. Measurement of the transition layer characteristics may be useful to control the surface treated by different methods. The authors believe the use of the method of invariants is promising in the metrology, including in the area of refractive index standard development.

Conflict of interest

The authors declare that they have no conflict of interest.

References

[1] D.B. Leviton, B.J. Frey. Proc. SPIE, **6273**, 62732K (2006). DOI: 10.1117/12.672853
[2] C.W. Wilmsen, H. Temkin, L.A. Coldren. Optics & Laser Technology, **32**, 293–296 (1999).
[3] C.F. Lin, B.L. Lee. Appl. Phys. Lett., **71**, 1598–1600 (1997). DOI: 10.1063/1.119844
[4] L. Kozlowski, G. Williams, G. Sullivan, C. Farley, R. Anderson, J. Chen, D. Cheung, W. Tennant, R. DeWames. IEEE Transactions on Electron Devices, **38**, 1124–1130 (1991). DOI: 10.1109/16.78388
[5] H. Cotal, C. Fetzer, J. Boisvert, G. Kinsey, R. King, P. Hebert, H. Yoon, N. Karam. Energy Environ. Sci., **2**, 174 (2009).
[6] G. Rempe, R.J. Thompson, H.J. Kimble, R. Lalezari. Opt. Lett., **17**, 363–365 (1992).
[7] A. Bruner, D. Eger, M.B. Oron, P. Blau, M. Katz. Opt. Lett., **28**, 194–196 (2003).
[8] K.A. Koç. Opt. Spectrosc., **127**, 1117–1121 (2019). DOI: 10.1134/S0030400X1912035X
[9] B.J.H. Stadler, J.P. Lorenzo. MRS Online Proceedings Library, **422**, 357–362 (1996). DOI: 10.1557/PROC-422-357
[10] El-Sayed El-Zaiat. Opt. Review, **21**, 54–59 (2014). DOI: 10.1007/s10043-014-0009-x
[11] S.V. Mutilin, T. Khasanov. Opt. Spectrosc., **105**, 461–465 (2008). DOI: 10.1134/S0030400X0809018X
[12] G.D. Pettit, W.J. Turner. J. Appl. Phys., **36**, 2081 (1965). DOI: 10.1063/1.1714410
[13] M.S. Whalen, J. Stone. J. Appl. Phys., **53**, 4340 (1982). DOI: 10.1063/1.331213
[14] V.A. Shvets, S.V. Rykhlitsky, I.Ya. Mittova, E.V. Tomina. ZhTF, **83** (11), 92 (2013) (in Russian).
[15] C.M. Herzinger, P.G. Snyder, B. Johs, J.A. Woollam. J. Appl. Phys., **77** (4), 1715 (1995).
[16] T.S. Chao, C.L. Lee, T.F. Lei. J. Materials Science Lett., **12**, 721 (1993).
[17] J.A. McCaulley, V.M. Donnelly, M. Vernon, I. Taha. Phys. Rev. B, **49** (11), 7408 (1994).
[18] Shyam Singh. Phys. Scr., **65**, 167 (2002).
[19] A.L. Briks. V kn.: *Issledovaniya v oblasti opticheskikh i svetovykh izmereniy. Trudy metrologicheskikh institutov SSSR* (Energiya, L., 1976), T. 193, s. 14–19 (in Russian).
[20] GOST 28869-90. *Mezhgosudarstvenny standart* IPK (Izdatelstvo standartov, M., 2005).
[21] L.A. Fedyukhin, A.V. Gorchakov, E.A. Kolosovsky. Pisma v ZhETF, **116** (5), 275 (2022) (in Russian). DOI: 10.31857/S1234567822170025
[22] L.A. Fedyukhin, A.V. Gorchakov, N.G. Korobeyschikov, I.V. Nikolaev. Pisma v ZhETF, **114** (5), 304 (2021) (in Russian). DOI: 10.31857/S1234567821170031
[23] M.M. Gorshkov. *Ellipsometriya* (Sovetskoe radio, M., 1974) (in Russian).
[24] F. Scandonne, L. Ballerini. Nuovo Cemento, **3**, 81 (1946). DOI: 10.1007/BF02858126
[25] N.I. Kalitievskiy. *Volnovaya optika* (Vyshaya shkola, M., 1995) (in Russian).
[26] L.A. Fedyukhin, A.V. Gorchakov, E.A. Kolosovsky. Opt. i spektr., **128**, 266 (2020) (in Russian). DOI: 10.21883/OS.2020.02.48975.219-19
[27] L.A. Fedyukhin, A.V. Gorchakov. ZhETF, **158** (5), 792 (2020) (in Russian). DOI: 10.31857/S0044451020110036

Translated by M.Verenikina